

De Novo Glutamine Synthesis: Importance for the Proliferation of Glioma Cells and Potentials for Its Detection With ^{13}N -Ammonia

Qiao He, MD¹, Xinchong Shi, MD¹, Linqi Zhang, MD², Chang Yi, MD¹, Xuezheng Zhang, MD¹, and Xiangsong Zhang, MD, PhD¹

Abstract

Purpose: The aim of this study was to investigate the role of de novo glutamine (Gln) synthesis in the proliferation of C6 glioma cells and its detection with ^{13}N -ammonia.

Methods: Chronic Gln-deprived C6 glioma (0.06C6) cells were established. The proliferation rates of C6 and 0.06C6 cells were measured under the conditions of Gln deprivation along with or without the addition of ammonia or glutamine synthetase (GS) inhibitor. ^{13}N -ammonia uptake was assessed in C6 cells by gamma counting and in rats with C6 and 0.06C6 xenografts by micro-positron emission tomography (PET) scanning. The expression of GS in C6 cells and xenografts was assessed by Western blotting and immunohistochemistry, respectively.

Results: The Gln-deprived C6 cells showed decreased proliferation ability but had a significant increase in GS expression. Furthermore, we found that low concentration of ammonia was sufficient to maintain the proliferation of Gln-deprived C6 cells, and ^{13}N -ammonia uptake in C6 cells showed Gln-dependent decrease, whereas inhibition of GS markedly reduced the proliferation of C6 cells as well as the uptake of ^{13}N -ammonia. Additionally, microPET/computed tomography exhibited that subcutaneous 0.06C6 xenografts had higher ^{13}N -ammonia uptake and GS expression in contrast to C6 xenografts.

Conclusion: De novo Gln synthesis through ammonia–glutamate reaction plays an important role in the proliferation of C6 cells. ^{13}N -ammonia can be a potential metabolic PET tracer for Gln-dependent tumors.

Keywords

de novo glutamine synthesis, C6, proliferation, ^{13}N -ammonia, glutamine synthetase

Introduction

Metabolic reprogramming has been recognized as a major hallmark of tumor, which is characterized by upregulated glycolysis and glutaminolysis, among others.¹ Glycolysis and glutaminolysis are 2 striking changes of tumor cellular bioenergetics.²⁻⁷ In comparison with normal cells, cancer cells prefer using glycolysis even in normoxic conditions. This metabolic alteration of cancer cells was called Warburg effect that paved the way for the development of ^{18}F -fluorodeoxyglucose positron emission tomography (^{18}F -FDG PET).^{7,8} Although most malignant tumors typically exhibited an increased uptake of ^{18}F -FDG, however, still a significant number of malignant tumors display hypometabolism on ^{18}F -FDG PET imaging. Besides, the main drawback of

^{18}F -FDG PET imaging is the lack of sufficient contrast due to high utilization of normal glucose in the brain.

¹ Department of Nuclear Medicine, the First Affiliated Hospital of Sun Yat-Sen University, Guangzhou, China.

² Department of Nuclear Medicine, the Cancer Center of Guangzhou Medical University, Guangzhou, China.

Submitted: 16/09/2015. Revised: 16/11/2015. Accepted: 23/02/2016.

Corresponding Author:

Xiangsong Zhang, Department of Nuclear Medicine, the First Affiliated Hospital of Sun Yat-Sen University, 58#, Zhongshan Er Road, Guangzhou 510080, China.

Email: sd_zh@163.net



In addition to glycolysis, many tumors also rely on glutaminolysis for survival.^{4-6,9} Glutaminolysis is a series of biochemical reactions catabolizing glutamine (Gln) into downstream metabolites such as glutamate (Glu) and α -ketoglutarate (α -KG). And α -KG then anaplerotically feeds into the tricarboxylic acid (TCA) cycle as a means of providing proliferating cells with biosynthetic intermediates and adenosine triphosphate (ATP).^{4,5} This upregulated tumor metabolism is useful for metabolic molecular imaging modality in the detection of tumor lesions. Novel metabolic PET tracers, such as L-[5-¹¹C]-glutamine and ¹⁸F-(2S, 4R) 4-fluoroglutamine, focused on glutaminolysis could provide valuable complement to ¹⁸F-FDG PET.^{10,11}

Although Gln is the most abundant amino acid in plasma,¹² the concentrations found in human plasma (0.6-1 mmol/L) are much lower than those commonly used in tissue culture media (2-4 mmol/L). Furthermore, the intratumor concentration of Gln could be much lower than that in plasma because of vascular and diffusional limitations. For these reasons, cells may be limited by the amount of Gln they are able to extract from the tumor microenvironment, and as a result, growth without dependence on a large Gln influx may give a selective advantage to tumor proliferation. As known, Gln could be synthesized from ammonia and Glu catalyzed by glutamine synthetase (GS; enzyme commission [EC] 6.3.1.2) that is the only known human enzyme catalyzing this reaction, and an increased expression of GS in response to the removal of Gln in culture medium has been shown in several tumor cell lines.¹³⁻¹⁵ We speculated that de novo Gln synthesis, in which ammonia is one of the major substrate, may provide Gln for glutaminolysis and play an important role in tumor cell proliferation. Hence, ¹³N-ammonia, a well-known PET tracer for myocardial blood flow, may be used as a metabolic PET tracer since it is a critical substrate for the synthesis of Gln. This study was to investigate the role of de novo Gln synthesis in C6 glioma cell proliferation and its potential detection with ¹³N-ammonia that is trapped in cells mainly through Gln synthesis reaction.¹⁶

Materials and Methods

Cell Culture

C6 glioma cells were purchased from American Type Culture Collection. Cells were cultured in Dulbecco Modified Eagle's Medium (Gibco, Grand Island, New York) supplemented with 10% fetal bovine serum (FBS; HyClone, Logan, Utah), 1% penicillin/streptomycin (Life Technologies, Carlsbad, California) at 37°C in a 5% CO₂ atmosphere in a humidified incubator.

Chronic Gln-deprived C6 glioma (0.06C6) cells were established from C6 cells subjected to a protocol of gradual Gln deprivation as described. C6 cells were serially passed through a medium containing 10% dialyzed FBS (dFBS; HyClone, Logan, Utah) and progressively decreased the Gln concentrations. At each passage, confluent dishes were harvested, and half of the cells were seeded into a dish containing a medium with a Gln concentration half of that in the preceding culture until cells growing in a Gln concentration of 0.06 mmol/L were obtained and deemed 0.06C6 cells.

Cell Proliferation Assay

C6 cells or 0.06C6 cells were plated in 96-well plates at densities of 2×10^6 cells/mL (100 μ L/well). Following 24 hours of attachment, the culture media were changed to Gln-free media supplemented with 10% dFBS plus various concentration of Gln (200 mmol/L; Gibco; 0, 0.05, 0.5, 1, 2, or 4 mmol/L) or ammonia (7.5 M; Gibco; 0, 0.5, 1, 2, 5, 10, and 15 mmol/L). Afterward, the cells were cultured in a medium containing 2 mmol/L L-methionine sulfoximine (L-MSO; Aladdin Inc, China), with cells growing in media without L-MSO serving as control groups. After the above treatment, cell proliferation was assayed by Cell Counting kit-8 (Dojindo Co, Japan).

Western Blotting

The cytoplasmic cell lysates obtained by radioimmunoprecipitation assay lysis buffer (Biocolor Co, China) were added in 2 \times sample buffer and heated for 5 minutes at 95°C. Samples were separated by 10% sodium dodecyl sulfate-polyacrylamide gel electrophoresis and transferred onto a polyvinylidene difluoride membrane. The membrane was blocked with 5% skim milk in phosphate buffer saline (PBS) containing 0.1% Tween-20 probed with mouse antibodies against anti-GS (1:500; BD Transduction Laboratories, South San Francisco, California) and peroxidase-conjugated affinity-pure anti-mouse immunoglobulin G secondary antibody (1:1000; Proteintech Group, Chicago). The membranes were stripped and reprobed with an anti- β -tubulin mouse monoclonal antibody (1:1000; Sigma, Saint Louis, Missouri) as a loading control. Protein bands were visualized with diaminobenzidine chromogenic substrate for peroxidase (horseradish peroxidase) detections.

Cell Uptake Assay

¹³N-ammonia was produced at our center by applying standard techniques and commercially available system for isotope generation (Ion Beam Applications; Cyclone-10, Belgium) as described previously.¹⁷ The radiochemical purity of ¹³N-ammonia was greater than 99%.

Cells were treated with medium containing serial concentrations of Gln with or without 2 mmol/L L-MSO. Two days later, the culture medium was removed and the attached cells were washed ($\times 3$) with ice-cold PBS. ¹³N-ammonia diluted with PBS was added to each well (37 kBq/mL/well), and the cells were incubated for 5 minutes at 37°C. Cellular uptake was stopped by removing medium from the cells and washing with ice-cold PBS. The cells were dissolved in 350 μ L of 1 N sodium hydroxide, and the radioactivity in cell lysate samples collected onto filter papers was measured using a gamma counter. One hundred microliters of the cell lysate were used for determination of the protein concentration by a modified Lowry protein assay. The data were normalized as percentage uptake of initial dose relative to 100 μ g of protein content.

Animal Model and MicroPET/Computed Tomography

The animal experiments followed the guidelines of the Institutional Animal Care and Use Committee of the First Affiliated Hospital of Sun Yat-Sen University.

Two Sprague-Dawley male rats weighing between 200 and 250 g were obtained from the Sun Yat-Sen University laboratory animal center, Guangzhou, China. C6 cells and 0.06C6 cells (5×10^6 , in a volume of 0.5 mL) were subcutaneously injected into the right foreleg and hind leg, respectively. They were scanned when the volume of subcutaneous xenografts had grown to above 250 mm³. With a slide caliper, xenograft volumes were determined by measurements of the larger tumor diameter (a) and the perpendicular diameter (b). The volume (V) was calculated with the following formula: $V = (a \times b^2)/2$.

The rats were placed under abdominal anesthesia by 10% chloral hydrate (4 mL/Kg) and injected intravenously (IV) with 1 mCi of ¹³N-ammonia. Computed tomography (CT) scanning was started immediately after the injection, then PET imaging was acquired after 10 minutes using a Siemens Inveon microPET camera (Siemens Medical Solutions, Knoxville, Tennessee). The emission protocol involved a 15-minute static scan. Body temperature of anesthetized animals in the scanner was kept at 33°C to 40°C, using heating plate. Radioactivity in tissues was measured and presented as the percentage injected dose per gram (%ID/g). Regions of interest were drawn around tumors (Ts) and the contralateral normal tissues (NTs), and the tumor-to-background ratios (T/NT) were calculated.

Immunohistochemistry

C6 glioma specimens were obtained after microPET/CT imaging. The tumor tissues were fixed in 4% paraformaldehyde and embedded in paraffin. Sections were cut at 4 μm thickness and incubated in 3% hydrogen peroxide for 10 minutes to block endogenous peroxidase. Subsequently, sections were incubated in 10% goat serum for 30 minutes at room temperature in order to block nonspecific binding. Afterward, sections were incubated overnight at 4°C with primary antibody (purified mouse anti-GS, 1:1000), then incubated with biotinylated secondary antibody (anti-mouse IgG, 1:500) followed by streptavidin biotin peroxidase complex (streptavidin biotin peroxidase complex immunohistochemical kit) for 30 minutes at room temperature. The immunoreaction was visualized using dolichos bifows agglutinin (DBA) chromogenic reagent kit for 10 minutes at room temperature. Finally, the sections were stained with hematoxylin.

Statistical Analysis

Each experiment was repeated at least in triplicate, and mean \pm standard deviation was calculated for each value. Statistical analysis of the results was performed using the Student *t* test and 1-way analysis of variance by SPSS13.0, followed by Dunnett multiple comparison test. A *P* value <.05 was considered significantly different.

Results

Proliferation of C6 Cells Is Gln Dependent

Gln dependency of C6 cells was demonstrated in Figure 1A and B, which shows bar charts and growth curves obtained for cells growing in the media containing various initial concentrations of Gln. Medium containing an initial concentration of 4 mmol/L supported rapid growth with a maximum cell proliferation. In contrast, little cell growth was supported by an initial Gln concentration of less than 0.25 mmol/L. To study the effect of Gln on C6 cells subjected to gradual Gln deprivation, which tumor in vivo would experience, controlled chronic Gln-deprived C6 glioma (0.06C6) cells were established, and the Gln dependency of 0.06C6 cells was examined by obtaining bar charts and growth curves for these cells grown in media containing various initial concentrations of Gln (Figure 1C and D). Compared to C6 cells, 0.06C6 cells exhibited a relatively Gln-independent growth.

Proliferation of C6 and 0.06C6 Cells Growing in Gln-Free Media Supported by Low Concentration of Ammonia and Reduced by GS Inhibitor L-MSO

To explore the role of de novo Gln synthesis from ammonia and Glu in C6 cell proliferation, we first examined the effect of ammonia on the viability and proliferation of cultured C6 and 0.06C6 cells plated in Gln-free media. The results showed that low concentration of ammonia is sufficient to maintain the survival and proliferation of C6 and 0.06C6 cells, and the optimal concentrations to their proliferation were 1 mmol/L and 2 mmol/L, respectively (Figure 2). A large amount of cells died in the media containing high concentrations of ammonia (Figure 2A). We next tested the effect of GS inhibition on the proliferation of C6 and 0.06C6 cells. Figure 3 shows that the cells grown in media with L-MSO had a significant lower proliferation, compared to that without L-MSO, and it was more obvious in 0.06C6 cells.

GS Expression Increases in C6 Cells in Response to Gln Deprivation

Western blotting analysis revealed that GS expression in C6 cells obviously increased in response to Gln deprivation, and it was negatively related to the Gln concentration in culture medium (Figure 4). Collectively, the results suggested that GS was upregulated in Gln-deprived C6 cells.

¹³N-Ammonia Uptake in C6 Cells Correlates With Gln Concentration and Is Inhibited by L-MSO

Then we explored the mechanism of ¹³N-ammonia trapping in tumor cells. ¹³N-ammonia uptake in C6 cells showed Gln-dependent decrease and almost completely inhibited by L-MSO (Table 1).

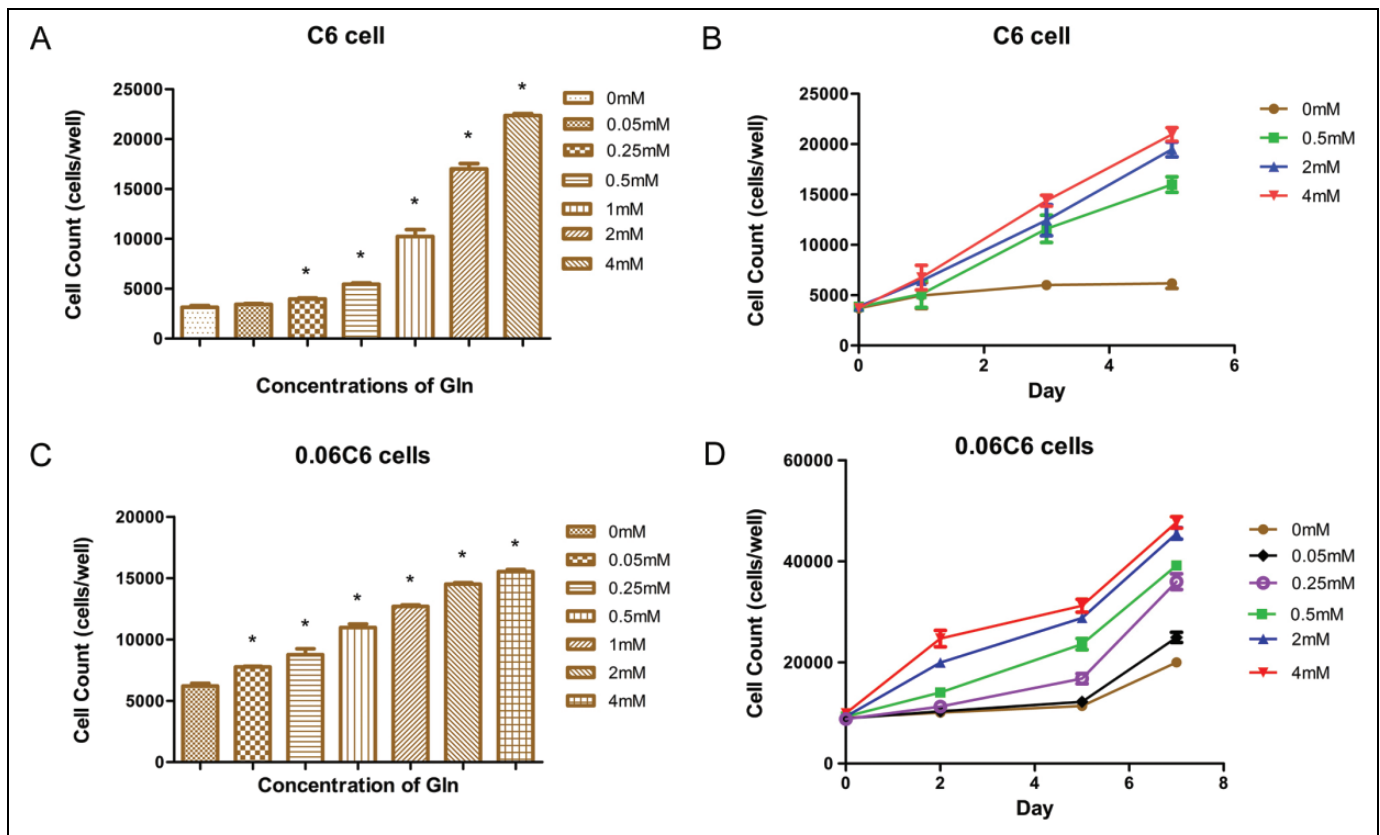


Figure 1. Role of glutamine (Gln) on the proliferation of C6 cells. Cell proliferation assays were performed on C6 cells (A and B) and 0.06C6 cells (C and D) 48 hours and several consecutive days after exposure to various concentration of Gln, respectively. Data points are the mean for more than triplicate determinations, with error bars representing standard deviations. Each bar represents the mean of 3 independent experiments. * $P < .05$.

0.06C6 Xenografts Have Higher Uptake of ^{13}N -Ammonia and More Expression of GS Than C6 Xenografts

To further evaluate the uptake of ^{13}N -ammonia in tumors in vivo, animal models with subcutaneous C6 and 0.06C6 xenografts were established. All the 4 xenografts showed a significant uptake of ^{13}N -ammonia (Figure 5A). ^{13}N -ammonia uptake in 0.06C6 xenografts was much higher than C6 xenografts, which resulted in very high tumor to background ratios (T/NT) (2.55 vs 2.84; 2.50 vs 3.88; Figure 5B). We examined GS expression in C6 and 0.06C6 xenografts using immunohistochemistry. The immunohistochemistry staining for GS showed that much more abundant GS-positive staining was observed in 0.06C6 sections compared to C6 sections, which demonstrated relatively higher expression of GS in C6 xenografts (Figure 5C).

Discussion

It has been demonstrated during the 1950s that Gln plays an essential role in cellular proliferation.¹⁸ Subsequent studies demonstrated that Gln not only is a major biosynthetic precursor serving as a carbon and nitrogen source, and an electron

donor, but also has an energetic function equally important to that of glucose during cellular proliferation.^{19,20} Furthermore, it has been shown that Gln, not glucose, is the major energy source for cultured hela cells, and series of cell lines have been proved to be Gln dependent.²¹ In this study, we demonstrated that C6 glioma cells are highly dependent on Gln in culture media. Low concentrations of ammonia could maintain the survival and proliferation of C6 cells in Gln-free medium, and the addition of L-MSO could inhibit the proliferation effectively. This indicates that de novo Gln is synthesized from ammonia and Glu for cell proliferation, in which GS is the key catalytic enzyme. So we suggest that coupling glutaminolysis and de novo Gln synthesis (ammonia-Glu-Gln axis) in C6 cells is the key to its growth and proliferation. The catalytic enzymes of ammonia-Glu-Gln axis are glutaminase (GLS) and GS. The mitochondrial GLS catalyze hydrolysis of Gln to ammonia and Glu (glutaminolysis). On the contrary, GS locates in cytoplasm to catalyze Gln synthesis with ammonia and Glu (de novo Gln synthesis). The regulation of GS has been well documented, and Gln deprivation is one of the most commonly reported factor for the regulation of GS expression as proved in this study.^{14,15,22}

The increasingly emerging evidence suggests that ammonia-Glu-Gln axis may play an important role in cancer

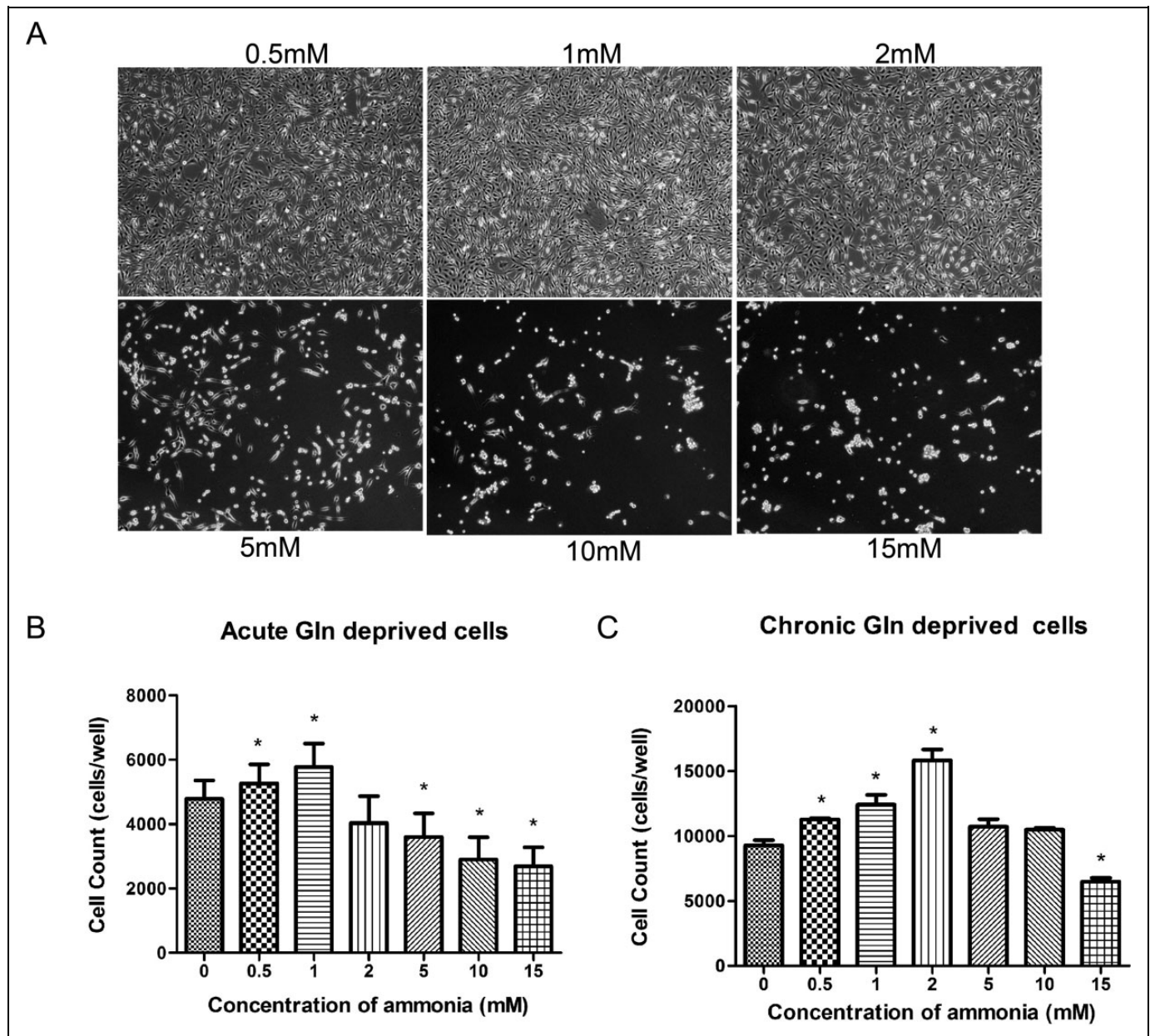


Figure 2. Effect of ammonia on the growth and proliferation of C6 and 0.06C6 cells in glutamine (Gln)-free media. (A) Micrographs of C6 cells were taken at $100\times$ magnification 48 hours after growth in Gln-free media with various concentration of ammonia. (B and C) Cell proliferation assays were performed on C6 cells and 0.06C6 cells 48 hours after growth in Gln-free media with various concentration of ammonia. Each bar represents the mean \pm standard deviation of 3 independent experiments. * $P < .05$.

biology. In addition to producing Gln for cancer metabolism, the metabolism axis can mediate the levels of ammonia. It is well known that hyperammonemia results in neurotoxicity through oxidative stress, the mitochondrial permeability transition, mitogen activated protein kinase (MAPK) and nuclear factor κ B, and the GS reaction in astrocyte protect ammonia neurotoxicity by converting excess ammonia and Glu into Gln.^{23,24} The similar mechanism may take place in the tumors with the increased glutaminolysis which generate ammonia. In this study, we observed that the de novo Gln synthesis plays a significant role in C6 cell proliferation through upregulation of

GS expression. The increased GS protein levels supported these cells to survive and grow in a Gln-deficient medium, and this compensated function was inhibited by specific GS enzyme inhibitor L-MSO.

With the consideration that de novo Gln synthesis may be a potential target for diagnosis and treatment of gliomas, it would be ideal if there is a mean to detect it in vivo in tumors noninvasively. ^{13}N -ammonia has long been proved to be a good circulatory PET tracer, since the small molecular weight makes it more sensitive for blood brain barrier (BBB) destruction of brain tumors.^{25,26} The ^{13}N -ammonia

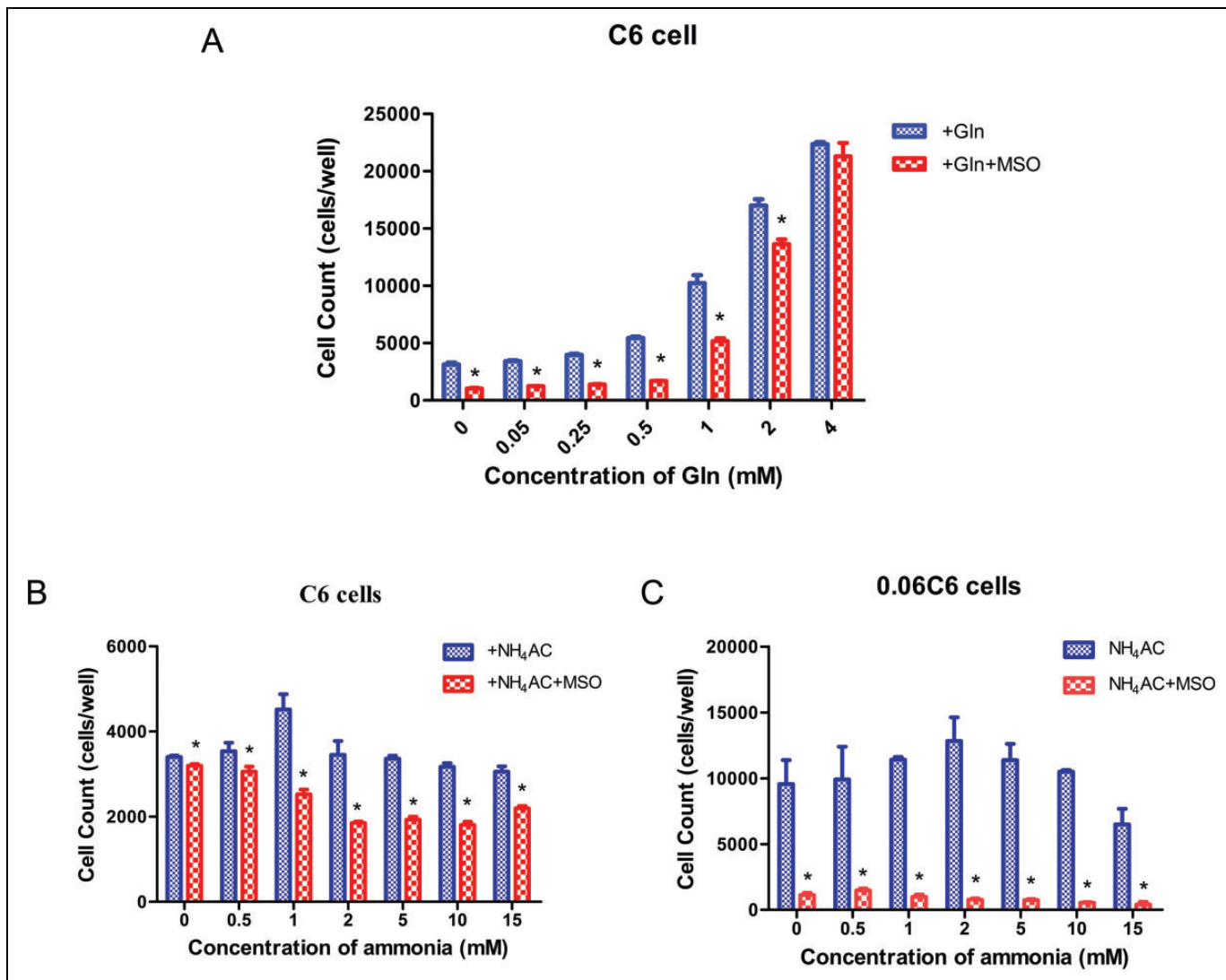


Figure 3. Effect of glutamine synthetase (GS) inhibition on the proliferation of C6 cells. Cell proliferation assays were performed on C6 cells (A) and 0.06C6 cells (B and C) 48 hours after culture in glutamine (Gln)-free media supplemented with 2 mmol/L L-methionine sulfoximine (L-MSO) and serials concentration of Gln or ammonia. The cells cultured in media without L-MSO served as control groups. Each bar represents the mean \pm standard deviation of 3 independent experiments. * $P < .05$.

extraction in brain tissues mainly depends on cerebral blood perfusion, capillary permeability–surface product, and the ammonia–Gln synthesis reaction.¹⁶ In the 1980s, Schelstraete et al reported that there was a substantial accumulation of ¹³N-ammonia in a series of malignant tumors, including breast cancer, soft tissue sarcomas, malignant lymphomas, and metastasis prostatic carcinoma.²⁷ Recently, Xiangsong et al reported that a relatively high uptake of ¹³N-ammonia was seen in cerebral astrocytomas and meningiomas, and that it has a potential value in the evaluation of brain tumors.^{17,28,29} Shi et al demonstrated that the uptake of ¹³N-ammonia in prostate cancers is related with GS expression.³⁰ But the mechanism of ¹³N-NH₃ used in tumor imaging is still not very clear. In this study, we observed the high uptake of ¹³N-ammonia in C6 cells and its xenografts in rats, and the uptake of ¹³N-ammonia in C6 cells decreased in a

Gln-dependent manner. What is more, this uptake could almost be completely inhibited by L-MSO. The xenografts originated from chronic Gln-deprived C6 glioma (0.06C6) cells that had the higher GS expression exhibited a higher uptake of ¹³N-ammonia than C6 xenografts. Glutamine synthetase is now the only known mammalian enzyme to catalyze the ATP-dependent condensation of ammonia and Glu to form Gln. These results suggest that ¹³N-ammonia is retained in C6 cells by the mechanism of de novo Gln synthesis, especially in the Gln-deficient tumors owing to higher GS expression, which may catalyze the synthesis of more Gln and make more ¹³N-NH₃ retain in cells.

Blood Gln concentration is much lower than that in the cell culture media, and vascular and diffusional limitations could further decrease the local Gln concentrations. Thus, as tumors grow and cause a chronic and progressive Gln deprivation, they

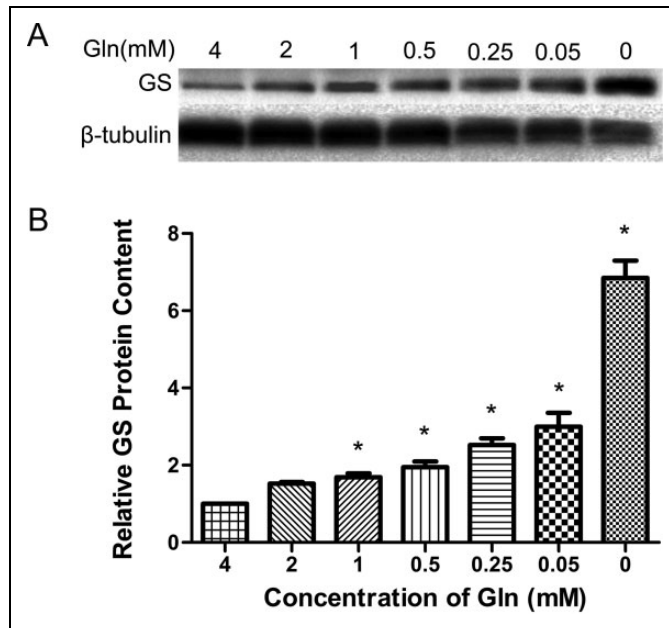


Figure 4. Glutamine synthetase (GS) expression of C6 cells in response to glutamine (Gln) deprivation. (A) GS protein synthesis in C6 cells was detected by Western blotting 48 hours after different levels of Gln deprivation. (B) Relative GS protein contents were calculated by Image lab software and normalized to the expressions of β -tubulin. Single samples were obtained and evaluated for each Gln concentration. Each bar represents the mean \pm standard deviation of 3 independent experiments. * $P < .05$.

Table 1. Uptake of ^{13}N Ammonia in C6 Cells: Gln-Dependent Decrease and Inhibition by L-MSO.

Group	Concentration of Gln (mmol/L) ^a	%ID/100 μgPro^b	
		-MSO	+MSO ^c
1.00	0	1.501 \pm 0.305	0.002 \pm 0.001
2.00	0.05	1.372 \pm 0.305	0.002 \pm 0.001
3.00	0.25	0.996 \pm 0.249	0.002 \pm 0.000
4.00	0.5	0.859 \pm 0.157	0.002 \pm 0.000
5.00	1	0.672 \pm 0.035	0.002 \pm 0.000
6.00	4	0.627 \pm 0.018	0.001 \pm 0.000

Abbreviations: Gln, glutamine; L-MSO, L-methionine sulfoximine.

^a The media used were Gln-free medium supplemented with the known concentration of Gln.

^b The values are means \pm standard deviation of 3 independent experiments with triplicate assays for each.

^c L-MSO, 2 mmol/L, was added to the media.

tend to adapt to a nutrient-poor intratumoral environment. Low extracellular Gln concentrations may restrict Gln influx into tumor cells, forcing cell metabolism to shift from glutaminolysis to Gln synthesis to replenish intracellular Gln pool. Although L-[5- ^{11}C]-glutamine and ^{18}F -(2S,4R)4-fluoroglutamine were recently developed for PET imaging of glutaminolysis in tumors,^{10,11,31} they cannot reflect the de novo Gln synthesis in tumors. ^{13}N -ammonia could provide a valuable complement to them.

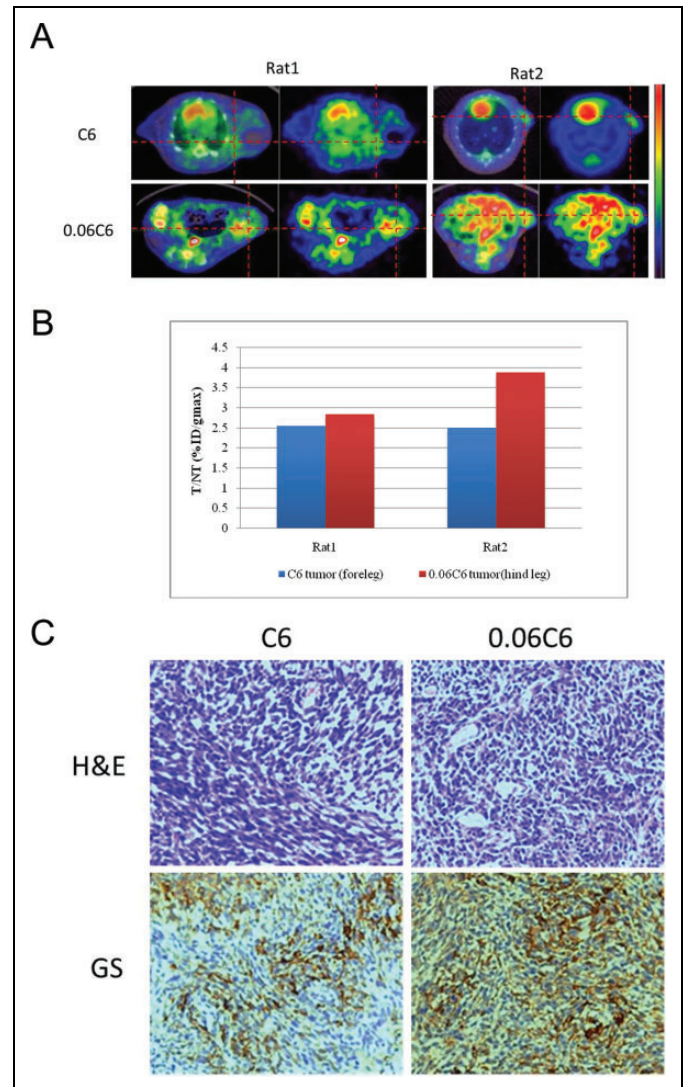


Figure 5. Micro-positron emission tomography/computed tomography (PET/CT) images obtained with rats bearing subcutaneous xenografts derived from C6 cells and 0.06C6 cells. (A) Representative decay-corrected transverse section microPET/CT images 10 minutes after intravenous injection of ^{13}N -ammonia (1 mCi per mouse). The subcutaneous xenografts are indicated by 2 crossed dotted red line. (B) The radioactivity ratios of xenografts to the contralateral normal tissue (T/NT) were based on the quantitative regions of interest (ROIs) analysis from ^{13}N -ammonia microPET/CT. (C) Hematoxylin and eosin (H&E) stains, glutamine synthetase (GS) in immunohistochemistry (IHC)

Conclusion

The results of this study show that the de novo Gln synthesis through ammonia-Gln reaction, which increases in response to Gln deprivation in media by upregulating GS expression, plays a significant role in C6 cell proliferation. ^{13}N -ammonia can be taken up by tumor cells through de novo Gln synthesis, and it may be useful as a novel metabolic PET tracer for tumor imaging for the study of a fundamental change in tumor metabolism with high-rate glutaminolysis, more sensitively for the Gln-deficient tumors.

Acknowledgments

The authors would like to thank Prof Guangmei Yan for providing laboratory equipment; Prof Wenbo Zhu and Dr Yuan Lin for their technical guidance.

Authors' Note

Qiao He and Xinchong Shi participated in most of the experiments, acquisition of data, data analysis, and drafting of the manuscript and revised it critically for important intellectual content. Linqi Zhang, Chang Yi, and Xuezhen Zhang participated in acquisition of data, data interpretation, data analysis, and animal experiments. Xiangsong Zhang participated in the conception and study design and critically revised the manuscript for important intellectual content and gave final approval of the version to be published. All authors have read and approved the final manuscript.

Declaration of Conflicting Interests

The author(s) declared no potential conflicts of interest with respect to the research, authorship, and/or publication of this article.

Funding

The author(s) disclosed receipt of the following financial support for the research, authorship, and/or publication of this article: This work was funded by National Natural Science Foundation (NSFC) of China Grant 81271599 and National Basic Research Program "973" of China Grant 2015CB755500.

References

- Hanahan D, Weinberg RA. Hallmarks of cancer: the next generation. *Cell*. 2011;144(5):646-674.
- Vander HM, Cantley LC, Thompson CB. Understanding the Warburg effect: the metabolic requirements of cell proliferation. *Science*. 2009;324(5930):1029-1033.
- DeBerardinis RJ, Lum JJ, Hatzivassiliou G, Thompson CB. The biology of cancer: metabolic reprogramming fuels cell growth and proliferation. *Cell Metab*. 2008;7(1):11-20.
- DeBerardinis RJ, Mancuso A, Daikhin E, et al. Beyond aerobic glycolysis: transformed cells can engage in glutamine metabolism that exceeds the requirement for protein and nucleotide synthesis. *Proc Natl Acad Sci U S A*. 2007;104(49):19345-19350.
- Wise DR, DeBerardinis RJ, Mancuso A, et al. Myc regulates a transcriptional program that stimulates mitochondrial glutaminolysis and leads to glutamine addiction. *Proc Natl Acad Sci U S A*. 2008;105(48):18782-18787.
- Dang CV. Glutaminolysis: supplying carbon or nitrogen or both for cancer cells? *Cell Cycle*. 2010;9(19):3884-3886.
- Dang CV. Rethinking the Warburg effect with Myc micromanaging glutamine metabolism. *Cancer Res*. 2010;70(3):859-862.
- Warburg O, Wind F, Negelein E. The metabolism of tumors in the body. *J Gen Physiol*. 1927;8(6):519-530.
- Hensley CT, Wasti AT, DeBerardinis RJ. Glutamine and cancer: cell biology, physiology, and clinical opportunities. *J Clin Invest*. 2013;123(9):3678-3684.
- Lieberman BP, Ploessl K, Wang L, et al. PET imaging of glutaminolysis in tumors by 18F-(2S,4R)-4-fluoroglutamine. *J Nucl Med*. 2011;52(12):1947-1955.
- Qu W, Oya S, Lieberman BP, et al. Preparation and characterization of L-[5-11C]-glutamine for metabolic imaging of tumors. *J Nucl Med*. 2012;53(1):98-105.
- Smith RJ, Wilmore DW. Glutamine nutrition and requirements. *JPEN J Parenter Enteral Nutr*. 1990;14(4 suppl):94S-99S.
- Crook RB, Tomkins GM. Effect of glutamine on the degradation of glutamine synthetase in hepatoma tissue-culture cells. *Biochem J*. 1978;176(1):47-52.
- Collins CL, Wasa M, Souba WW, Abcouwer SF. Regulation of glutamine synthetase in human breast carcinoma cells and experimental tumors. *Surgery*. 1997;122(2):451-463, discussion 463-464.
- Lacoste L, Chaudhary KD, Lapointe J. Derepression of the glutamine synthetase in neuroblastoma cells at low concentrations of glutamine. *J Neurochem*. 1982;39(1):78-85.
- Phelps ME, Huang SC, Hoffman EJ, Selin C, Kuhl DE. Cerebral extraction of N-13 ammonia: its dependence on cerebral blood flow and capillary permeability-surface area product. *Stroke*. 1981;12(5):607-619.
- Xiangsong Z, Weian C, Dianchao Y, Xiaoyan W, Zhifeng C, Xiongchong S. Usefulness of (13)N-NH (3) PET in the evaluation of brain lesions that are hypometabolic on (18)F-FDG PET. *J Neurooncol*. 2011;105(1):103-107.
- Eagle H, Oyama VI, Levy M, Horton CL, Fleischman R. The growth response of mammalian cells in tissue culture to L-glutamine and L-glutamic acid. *J Biol Chem*. 1956;218(2):607-616.
- Brand K. Glutamine and glucose metabolism during thymocyte proliferation. Pathways of glutamine and glutamate metabolism. *Biochem J*. 1985; 228:353-61.
- Zielke HR, Zielke CL, Ozand PT. Glutamine: a major energy source for cultured mammalian cells. *Fed Proc*. 1984;43(1):121-125.
- Reitzer LJ, Wice BM, Kennell D. Evidence that glutamine, not sugar, is the major energy source for cultured HeLa cells. *J Biol Chem*. 1979;254(8):2669-2676.
- Feng B, Shiber SK, Max SR. Glutamine regulates glutamine synthetase expression in skeletal muscle cells in culture. *J Cell Physiol*. 1990;145(2):376-380.
- Norenberg MD, Rama RK, Jayakumar AR. Signaling factors in the mechanism of ammonia neurotoxicity. *Metab Brain Dis*. 2009;24(1):103-117.
- Suarez I, Bodega G, Fernandez B. Glutamine synthetase in brain: effect of ammonia. *Neurochem Int*. 2002;41(2-3):123-142.
- Teragawa H, Morita K, Shishido H, et al. Impaired myocardial blood flow reserve in subjects with metabolic syndrome analyzed using positron emission tomography and N-13 labeled ammonia. *Eur J Nucl Med Mol Imaging*. 2010; 37(2):368-376.
- Burkhard N, Herzog BA, Husmann L, et al. Coronary calcium score scans for attenuation correction of quantitative PET/CT 13N-ammonia myocardial perfusion imaging. *Eur J Nucl Med Mol Imaging*. 2010;37(2):517-521.
- Schelstraete K, Simons M, Deman J, et al. Uptake of 13N-ammonia by human tumours as studied by positron emission tomography. *Br J Radiol*. 1982;55(659):797-804.

28. Xiangsong Z, Changhong L, Weian C, Dong Z. PET Imaging of cerebral astrocytoma with ^{13}N -ammonia. *J Neurooncol.* 2006; 78(2):145-151.
29. Xiangsong Z, Xingchong S, Chang Y, Xiaoyan W, Zhifeng C. ^{13}N - NH_3 versus F-18 FDG in detection of intracranial meningioma: initial report. *Clin Nucl Med.* 2011;36(11): 1003-1006.
30. Shi X, Zhang X, Yi C, Liu Y, He Q. [^{13}N]Ammonia Positron Emission Tomographic/Computed Tomographic Imaging Targeting Glutamine Synthetase Expression in Prostate Cancer. *Mol Imaging.* 2014;13:1-10.
31. Wu Z, Zha Z, Li G, et al. [^{18}F](2S,4S)-4-(3-Fluoropropyl)glutamine as a tumor imaging agent. *Mol Pharm.* 2014;11(11): 3852-3866.